IAI Journals.ASM.org

Interplay between Manganese and Iron in Pneumococcal Pathogenesis: Role of the Orphan Response Regulator RitR

Cheryl-Lynn Y. Ong,[a] Adam J. Potter,[b] Claudia Trappetti,[b] Mark J. Walker,[a] Michael P. Jennings,[c] James C. Paton,[b] Alastair G. McEwan[a]

School of Chemistry and Molecular Biosciences and Australian Infectious Diseases Research Centre, University of Queensland, Brisbane, Queensland, Australia[a]; Research Centre for Infectious Diseases, School of Molecular and Biomedical Science, University of Adelaide, Adelaide, South Australia[b]; Institute for Glycomics, Griffith University, Queensland, Australia[c]

***Streptococcus pneumoniae* (the pneumococcus) is a major human pathogen that is carried asymptomatically in the nasopharynx by up to 70% of the human population. Translocation of the bacteria into internal sites can cause a range of diseases, such as pneumonia, otitis media, meningitis, and bacteremia. This transition from nasopharynx to growth at systemic sites means that the pneumococcus needs to adjust to a variety of environmental conditions, including transition metal ion availability. Although it is an important nutrient, iron potentiates oxidative stress, and it is established that in *S. pneumoniae*, expression of iron transport systems and proteins that protect against oxidative stress are regulated by an orphan response regulator, RitR. In this study, we investigated the effect of iron and manganese ion availability on the growth of a *ritR* mutant. Deletion of *ritR* led to impaired growth of bacteria in high-iron medium, but this phenotype could be suppressed with the addition of manganese. Measurement of metal ion accumulation indicated that manganese prevents iron accumulation. Furthermore, the addition of manganese also led to a reduction in the amount of hydrogen peroxide produced by bacterial cells. Studies of virulence in a murine model of infection indicated that RitR was not essential for pneumococcal survival and suggested that derepression of iron uptake systems may enhance the survival of pneumococci in some niches.**

Streptococcus pneumoniae (the pneumococcus) continues to be responsible for massive global morbidity and mortality, causing more deaths worldwide than any other single pathogen (1). It is carried asymptomatically in the nasopharynx of a high proportion of the human population, but in a subset of these individuals, it translocates to deeper sites, causing a broad spectrum of diseases, including pneumonia, meningitis, bacteremia, and otitis media (2). In developing countries, 1 to 2 million children under 5 years of age die each year from pneumonia, of which *S. pneumoniae* is the single most common cause, accounting for 20 to 25% of all deaths in this age group (3, 4). Even in developed countries, where effective antimicrobial therapy is readily accessible, morbidity and mortality are substantial. In these countries, deaths from pneumococcal disease occur primarily among those over 60 years of age, with case fatality rates of 10 to 20% for pneumonia and up to 60% for bacteremia (4).

Although it is recognized that the host niches occupied by *S. pneumoniae* differ greatly, there is still a lack of information about the effect of a changing microenvironment on the physiological properties of the bacterium and how this relates to pathogenesis. Over the last decade, the importance of transition metal ions in host-pathogen interactions has been recognized, with manganese emerging as a transition metal ion of particular importance to the cellular physiology of the pneumococcus (5, 6). This ion is a prosthetic group in superoxide dismutase (SodA) and also has been shown to have direct antioxidant properties (7, 8). Also, CpsB, a protein that is essential for the cycle of polysaccharide capsule assembly, export, and attachment to the cell wall, is a manganese-dependent tyrosine phosphatase (9). Manganese is present at low concentrations in host tissues (range, 0.4 to 1.1 μM in the blood, nasopharynx, and lungs of mice) (10), and transport of manganese is dependent on the ABC-type permease PsaBCA (11). The correlation of hypersensitivity of *psa* mutants of *S. pneumoniae* to oxidative stress with loss of ability to transport manganese explains the avirulence of pneumococcal *psa* mutants in murine models (5, 8).

Even though *S. pneumoniae* lacks a respiratory chain, it can tolerate and consume oxygen. Two enzymes are of particular importance: NADH oxidase, which reduces molecular oxygen to water and consumes NADH produced during glycolysis (12–14), and pyruvate oxidase (SpxB), which converts pyruvate to acetyl-phosphate and hydrogen peroxide (H_2O_2) (15, 16). The actions of these enzymes provide the pneumococcus with an increased yield of ATP per mole of glucose. However, the H_2O_2 that is generated has the potential to cause oxidative damage to the bacterium. The pneumococcus lacks catalase, but it does possess a thiol-peroxidase (PsaD) (5, 8). Manganese plays a pivotal role in the defense of the cell against peroxide stress, although the biochemical basis for its action is still a matter of intensive study (17–19). An important factor in the protection of *S. pneumoniae* against peroxide stress is the relatively low requirement for iron; the pneumococcus has only a few enzymes containing iron-sulfur clusters, and it lacks a respiratory chain (20–22). Thus, the potential for production of damaging hydroxyl radicals from reaction of ferrous ions (Fe^{2+}) and hydrogen peroxide (the Fenton reaction) is reduced. Nevertheless, *S. pneumoniae* does possess a Dpr protein (Dps-like per-

Received 31 July 2012 Returned for modification 3 September 2012
Accepted 17 November 2012
Published ahead of print 26 November 2012
Editor: S. M. Payne
Address correspondence to Alastair G. McEwan, mcewan@uq.edu.au.

doi:10.1128/IAI.00805-12

TABLE 1 Strains used in the study

Strain	Description	Reference
D39	*S. pneumoniae* virulent type 2 strain	22
D39 Δ*ritR*	*S. pneumoniae* D39 *ritR*::*erm* deletion mutant	This study
D39 Δ*ritR* Δ*sodA*	*S. pneumoniae* D39 *ritR*::*erm* and *sodA*::*aad* double-deletion mutant	This study
D39 Δ*ritR*::*ritR*	*S. pneumoniae* D39 *ritR* complemented strain	This study

TABLE 2 Primers used in the study

Primer	Sequence (5′–3′)
ritR1	5′-TCAAAGAAGTGCCAGTCGTG
ritR2	5′-TTGTTCATGTAATCACTCCTTCTTCCC CATGGCTGACCTAC
ritR3	5′-CGGGAGGAAATAATTCTATGAGCCATG CAAGAATAGAAAAGCA
ritR4	5′-GGTCGTATTCACTGCCAAGG
ery-F	5′-GAAGGAGTGATTACATGAACAA
ery-R	5′-CTCATAGAATTATTTCCTCCCG
sodA1	5′-GGATGTGGAACTGGAGTTGG
sodA2	5′-CGTATGTATTCAAATATATCCTCCTCG CCATCTGTAATACCTCTTTTTCTTT
sodA3	5′-TAACTATAAACTATTTAAATAACAGAT TTGATAGTTGGAGGGAAGAATTG
sodA4	5′-ACAGTCGACCTGAGTGGTCA
spec-F	5′-GAGGAGGATATATTTGAATACATACG
spec-R	5′-AATCTGTTATTTAAATAGTTTATAGTTA
16S-R	5′-AAGCAACGCGAAGAACCTTA
16S-R	5′-ACCACCTGTCACCTCTGTCC
ritR-F	5′-ATCCGCTATCTACGGAGCAA
ritR-R	5′-TATCCAACACCACGCACAGT
gnd-F	5′-AAAGATCCGTCAAGCCCTTT
gnd-R	5′-GCTACACGCAATTGAGCAAA
psaA-F	5′-TGGTGTTCCAAGTGCCTACA
psaA-R	5′-TTTGGCGAAGTTTTTCAACC
psaD-F	5′-CAAGGCGCTTGATTTTTCTC
psaD-R	5′-TTGAGCAGATGCCTGTATCG
zwf-F	5′-ATTGAAAAGCTCTGGGCTGA
zwf-R	5′-GTCAAAGCTGGCTTGAGGTC
spxB-F	5′-TTCAAACTTCGCATTTGCTG
spxB-R	5′-AGGGCATGACGTTTACCAAG

oxide resistance protein) that, like its *Escherichia coli* homologue (Dps), is able to protect the cell against iron and peroxide stress (23, 24). The response regulator RitR has previously been identified as being central to the response to iron and oxidative stress by regulating expression of *dpr* and repressing expression of iron uptake systems in *S. pneumoniae* (25).

In the present study, we investigated the effect of mutation of *ritR* on pneumococcal growth and physiology in media with differing Fe/Mn ratios. Furthermore, we compared the pathogenesis properties of the virulent encapsulated strain D39 and an isogenic *ritR* mutant using a murine model of infection. These observations provide new insights into the interplay between transition metal ions in pneumococcal survival and virulence.

MATERIALS AND METHODS

Bacterial strains and growth conditions. The virulent *S. pneumoniae* type 2 strain D39 (NCTC 7466) and derived strains were routinely grown in liquid culture at 37°C in chemically defined medium (CDM) (26). The strains used in this study are listed in Table 1. CDM was modified to include 4 mM L-lactate and 10 mM D-glucose as carbon sources, to exclude iron to derive Mn-CDM (final Mn concentration, 33 μM), and to exclude manganese to derive Fe-CDM (final Fe concentration, 20 μM). Cells were plated on blood agar base (Becton, Dickinson) supplemented with 5% defibrinated horse blood (blood agar plates) and grown at 37°C in the presence of 5% CO_2. When antibiotic selection was required, media were supplemented with 0.2 μg/ml erythromycin or 200 μg/ml spectinomycin. For mouse challenge experiments, strains were cultured in nutrient broth supplemented with 10% horse serum (serum broth).

DNA manipulation and genetic techniques. Chromosomal DNA was purified by using the GenElute bacterial genomic DNA kit (Sigma). PCR was performed by using Kod Hot Start DNA polymerase (Merck) (for amplification of the *ritR* deletion fragments) or *Taq* polymerase (New England BioLabs) (for screening assays) according to the manufacturers' instructions. *S. pneumoniae* D39 Δ*ritR* was constructed by deletion-replacement using overlap extension PCR mutagenesis and direct transformation as previously described (27). The 1-kb region upstream of *ritR* was amplified using primers ritR1 and ritR2, while the 1-kb region downstream of *ritR* was amplified using primers ritR3 and ritR4. The erythromycin cassette was amplified using primers ery-F and ery-R. The three PCR fragments generated were joined together using primers ritR1 and ritR4 to form the deletion fragment. The *ritR* and *sodA* double deletion was constructed using a similar method. The 1-kb region upstream of *sodA* was amplified using primers sodA1 and sodA2, while the 1-kb region downstream of *sodA* was amplified using primers sodA3 and sodA4. The spectinomycin cassette was amplified using primers spec-F and spec-R. All deletion mutants were confirmed by Sanger sequencing. The primer sequences used in this study are listed in Table 2.

Complementation of D39Δ*ritR* was performed by marker rescue. The entire region, including the 1-kbp regions upstream and downstream of *ritR*, was amplified using primers ritR1 and ritR4. The purified PCR fragment was transformed into D39 Δ*ritR* (27), and potential complemented strains were screened for the loss of erythromycin resistance. Erythromycin-sensitive colonies were screened by PCR, and the *ritR* complemented strain was confirmed via Sanger sequencing. All samples were submitted to the Australian Equine Genome Research Centre (University of Queensland, Brisbane, Australia) for Sanger sequence analysis.

Growth curve analysis. Cells were grown overnight in CDM, washed three times in phosphate buffer, and diluted to an optical density at 600 nm (OD_{600}) of 0.01 in fresh medium. The cells were statically grown in a microaerobic environment (25 ml medium in a 50-ml tube). The OD_{600} of the cells was measured every hour initially, increasing to every half hour during the exponential phase.

Hydrogen peroxide concentration measurement. Cells were grown microaerobically in CDM to mid-exponential phase (OD_{600}, ~0.6). The cells were pelleted by centrifugation, and the supernatant was filtered through a 0.22-μm filter. Hydrogen peroxide was detected in the filtered supernatant in accordance with the Amplex Red hydrogen peroxide/peroxidase assay kit (Invitrogen). The final value was normalized to the number of cells present by measuring the total protein content in accordance with the QuantiPro BCA assay kit (Sigma) instructions.

Quantitative gene expression studies. RNA was isolated from 5 ml of cells harvested at the desired growth phase in accordance with the RNeasy Minikit (Qiagen). The isolated RNA was DNase treated using the RNase-Free DNase set (Qiagen) and quantified using a Nanodrop instrument (Thermo Scientific). One microgram of RNA was converted to cDNA using the SuperScript III first-strand synthesis system for reverse transcriptase (RT)-PCR (Invitrogen). Real-time reverse transcriptase PCR was performed on the 1:5-diluted cDNA using the following primers: 16S-F, 16S-R, ritR-F, ritR-R, gnd-F, gnd-R, psaA-F, psaA-R, psaD-F, psaD-R, zwf-F, zwf-R, spxB-F, and spxB-R. The primer sequences used in this study are listed in Table 2. The PCR was performed using SYBR green Master Mix (Applied Biosystems) according to the manufacturer's instructions. The reaction was performed using a 7900 HT real-time PCR machine (Applied Biosystems) under the following conditions: 95°C for

10 min; 40 cycles of 95°C for 15 s and 60°C for 1 min; and a final dissociation cycle of 95°C for 2 min, 60°C for 15 s, and 95°C for 15 s. All data were analyzed using SDS 2.2.2 software (Applied Biosystems). Relative gene expression was calculated using the $2^{-\Delta CT}$ method with 16S as the reference gene.

Murine model of infection. For mouse survival experiments, 10 5- to 6-week-old outbred female CD1 (Swiss) mice (per strain) were injected intraperitoneally with 5×10^3 CFU of either D39 wild-type (WT), D39 Δ*ritR*, or complemented cells; the mice were observed over 8 days; and survival times were recorded. For the intranasal-challenge experiments, 20 mice (per strain) were first anesthetized by intraperitoneal injection with pentobarbitone sodium (Nembutal; Rhone-Merieux) before 5×10^6 CFU of the D39 WT, D39 Δ*ritR*, or *ritR* complemented strain was pipetted into the nares and involuntarily inhaled. Ten mice (per strain) were euthanized at 24 h and 48 h postchallenge, and the numbers of viable cells in the blood, lungs, nasal wash, and nasal tissue were determined as follows. Blood (1 ml) was collected from the heart, the nasopharynx was washed with 1 ml phosphate-buffered saline (PBS), and the lungs and the nasopharyngeal cavity were excised, washed briefly, placed in 1 ml of sterile PBS, and homogenized using a Precellys 24 homogenizer (Bertin Technologies). Samples were then serially diluted and plated on blood agar (supplemented with 0.2 μg/ml erythromycin where needed) to determine the numbers of viable D39 WT, D39 Δ*ritR*, and *ritR* complemented cells. All animal experiments were conducted according to the Guidelines for the Care and Use of Laboratory Animals (National Health and Medical Research Council, Canberra, Australia) and were approved by the University of Adelaide Animal Ethics Committee.

Analysis of the intracellular metal concentration. Cells harvested from the desired growth phase were pelleted and washed with phosphate buffer, resuspended in 80% nitric acid, and incubated at 80°C for 24 h. The sample was then diluted to 2% nitric acid and submitted for inductively coupled plasma mass spectrometry (ICP-MS) analysis at the National Research Centre for Environmental Toxicology (University of Queensland, Brisbane, Australia). The final value was normalized to the number of cells present by measuring the total protein content in accordance with the QuantiPro BCA assay kit (Sigma) instructions.

Statistical analysis. Differences in metal ion concentrations, hydrogen peroxide concentrations, relative gene expression, and numbers of CFU/ml in mouse studies were analyzed using a two-tailed *t* test (Minitab 15 statistical software).

RESULTS

Analysis of the growth of the *ritR* mutant in media containing altered Fe/Mn ratios. To determine whether the Fe/Mn ratio influenced the growth of *S. pneumoniae*, we developed two media based on a CDM (26). One of them had a high Fe/Mn ratio (Fe-CDM), while the other had a low Fe/Mn ratio (Mn-CDM) (see Materials and Methods). Figure 1A shows that the growth curves for wild-type D39 and the *ritR* mutant in Mn-CDM were essentially the same. However, in Fe-CDM, growth of the wild-type strain was unaffected, but the *ritR* mutant did not emerge from lag phase and did not grow in this high-Fe/Mn medium. Complementation of the *ritR* mutant restored its ability to grow in Fe-CDM (Fig. 1A), confirming that the phenotype of the mutant is attributable to the *ritR* mutation.

The above data confirmed previous work (25) showing that the *ritR* mutant is unable to tolerate high Fe levels. To determine whether Mn could influence this loss of Fe tolerance, we titrated Mn into Fe-CDM and tested growth as a function of the Fe/Mn ratio. Figure 1B shows that increasing Mn restored growth of the *ritR* mutant in Fe-CDM. The molecular basis of the protection afforded to bacteria by manganese is still not fully understood, although two interesting hypotheses have emerged that may explain its antioxidant activity (18, 28), in addition to its role as a component of Mn-dependent superoxide dismutases and catalases. *S. pneumoniae* possesses an Mn-dependent superoxide dismutase (SodA), but not an Mn-dependent catalase. To investigate whether SodA contributed to the rescue of the *ritR* mutant by Mn, we constructed a *ritR sodA* double mutant. Figure 1C shows that

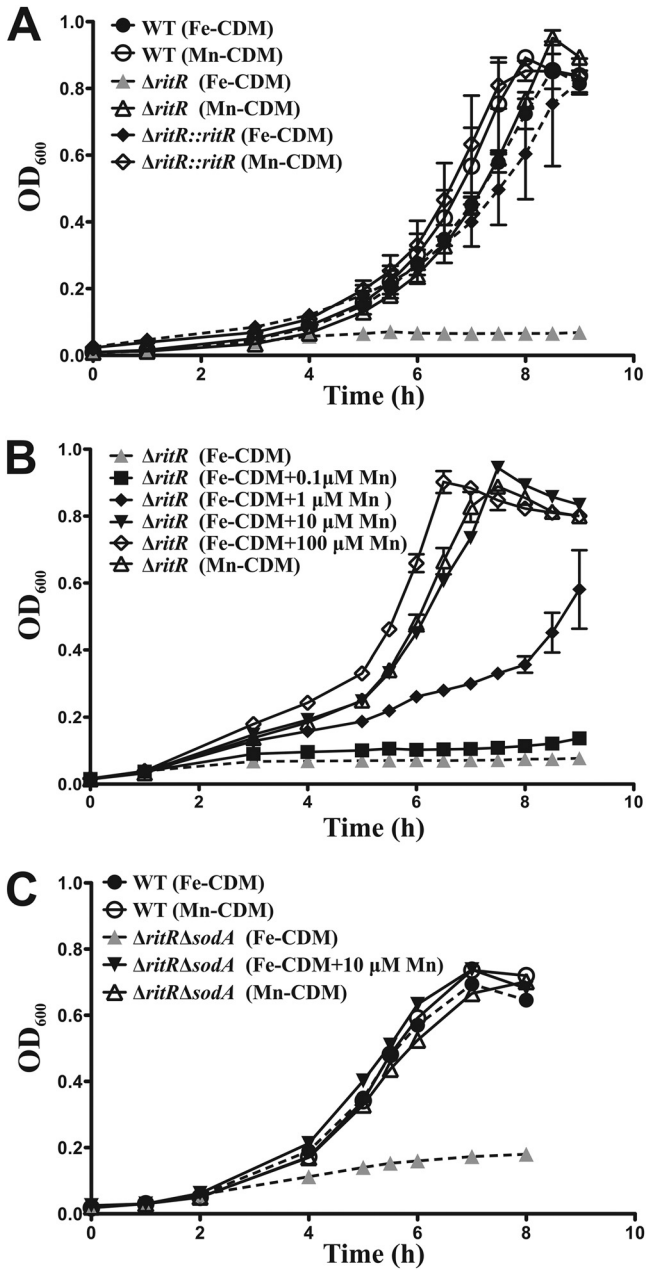

FIG 1 Comparison of the growth curve analyses of D39 WT, isogenic deletion mutant (Δ*ritR*), and complemented (Δ*ritR*::*ritR*) strains. (A) Growth of the WT in Fe-CDM and Mn-CDM compared to that of the Δ*ritR* strain in Fe-CDM and Mn-CDM and the Δ*ritR*::*ritR* strain in Fe-CDM and Mn-CDM. (B) Growth of the Δ*ritR* strain in Mn-CDM and Fe-CDM with the addition (+) of 0.1, 1, 10, and 100 μM Mn. (C) Growth of the WT in Fe-CDM and Mn-CDM compared tothat of a Δ*ritR* Δ*sodA* double-deletion mutant in Fe-CDM and Mn-CDM and Fe-CDM supplemented with 10 μM Mn, demonstrating that Mn rescue is independent of SodA activity. The error bars indicate the standard deviations of three independent experiments.

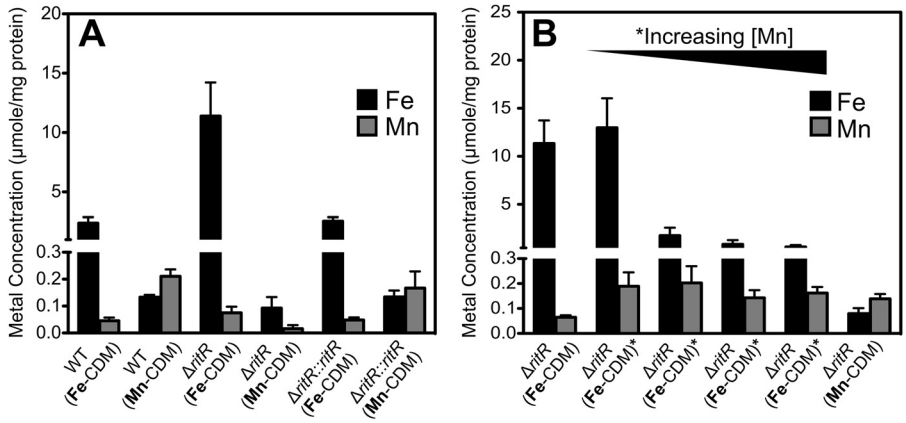

FIG 2 Accumulation of Fe and Mn in pneumococcal cells grown in different growth media. (A) Internal Fe/Mn ratio of D39 WT, isogenic deletion mutant (Δ*ritR*), and complemented (Δ*ritR*::*ritR*) strains when grown in Fe-CDM compared to Mn-CDM. (B) Internal Fe/Mn ratio of the D39 Δ*ritR* strain when grown in Mn-CDM and Fe-CDM supplemented with 0.1, 1, 10, and 100 μM Mn. The results are shown as averages of three independent experiments, and the results were normalized with the cellular protein concentration. Samples were collected during the exponential phase of growth, with the exception of the Δ*ritR* strain when grown in Fe-CDM (the sample was collected during the lag phase of growth). The error bars indicate the standard deviations of three independent experiments.

addition of Mn to the Fe-CDM still rescued this double mutant from Fe-induced growth inhibition, indicating that the removal of superoxide by SodA is not a factor in the Mn-dependent suppression of Fe-induced stress.

Effect of Mn on the intracellular Fe concentration. To further understand the biochemical basis of the Mn-dependent rescue of the *ritR* mutant from Fe-induced stress, we determined the cellular content of these two metal ions using ICP-MS. Cells were collected during mid-exponential phase and prepared for ICP-MS analysis as described in Materials and Methods. However, due to the inability of the *ritR* mutant to grow beyond an OD_{600} of 0.1 in Fe-CDM, a larger volume of cells was collected during mid-lag phase, and all the results were adjusted based on the amount of protein present per sample. Figure 2A shows that in the wild-type and *ritR* complemented strains, the concentration of Fe in cells grown in Fe-CDM was about 20-fold higher than that observed for cells grown in Mn-CDM. However, this was only a small increase compared to the situation for the *ritR* mutant, where it was observed that a higher concentration of Fe had accumulated in cells grown in Fe-CDM (>120-fold increase). Thus, the *ritR* mutant hyperaccumulates Fe, consistent with previous observations that this response regulator is a repressor of the expression of iron uptake systems in *S. pneumoniae* (25). We also investigated the effect of increasing Mn on the cellular concentrations of Fe and Mn in the *ritR* mutant grown in Fe-CDM. Figure 2B shows that addition of a minimum of 1 μM Mn resulted in a significant decrease in Fe accumulation (from 11 to 2 μmol/mg protein; $P < 0.001$). Furthermore, Fe accumulation decreased even further to 0.8 μmol/mg protein as added Mn was increased to 10 μM, although this did not reach statistical significance ($P > 0.05$). Subsequently, the internal Fe level remained low at around 0.6 to 0.7 μmol/mg protein when the added Mn was further increased to 100 μM ($P > 0.05$). Thus, it can be concluded that the Mn-dependent rescue of the *ritR* mutant from Fe-induced stress is correlated with a decrease in the cellular Fe content.

Effect of Mn on hydrogen peroxide production. Hydrogen peroxide is produced by the pneumococcus as a consequence of the action of pyruvate oxidase (SpxB) (15). In cells grown in Mn-CDM, the wild-type, *ritR* mutant, and complemented *ritR* mutant produced similar amounts of hydrogen peroxide (1.4, 1.1, and 1.3 μmol per mg protein, respectively; $P > 0.05$) (Fig. 3A). However, in Fe-CDM, hydrogen peroxide production was much higher in the *ritR* deletion mutant than in the wild type and the complemented *ritR* mutant (23.0 compared to 1.4 and 1.6 μmol per mg protein, respectively; $P = 0.0001$) (Fig. 3A). Addition of as little as 10 μM Mn to Fe-CDM resulted in a decrease in hydrogen peroxide production in the mutant ($P < 0.05$) (Fig. 3B), with further reduction achieved at higher Mn concentrations ($P < 0.05$) (Fig. 3B).

Effect of differing Fe/Mn ratios on the gene expression profile of *S. pneumoniae*. In order to begin to understand the physiological basis of the protective effects of manganese, samples were collected during the mid-exponential phase of growth in either Fe-CDM or Mn-CDM, with the exception of the *ritR* mutant in Fe-CDM, where a larger volume of sample was collected during the mid-lag phase of growth, and relative gene expression was measured. Expression of the following genes was tested: *ritR*, *spxB*, *gnd*, *zwf*, *psaA*, and *psaD*, which encode RitR, pyruvate oxidase, 6-phosphogluconate dehydrogenase, glucose-6-phosphate dehydrogenase, pneumococcal surface adhesin A (manganese ABC transporter), and a putative thiol peroxidase, respectively. *ritR* was expressed at an approximately 2-fold-higher level when the cells were grown in a high-Fe environment compared to a high-Mn environment ($P < 0.05$) (Fig. 4A). This was consistent with previous studies indicating that *ritR* is upregulated by Fe (25).

Hydrogen peroxide is produced by the actions of two enzymes, lactate oxidase (LctO) and pyruvate oxidase (SpxB). As shown in Fig. 3A, it was observed that hydrogen peroxide levels were significantly higher in the *ritR* mutant when grown in Fe-CDM. The gene expression levels of *lctO* showed no significant difference in all strains when grown in either medium (data not shown). However, the gene expression of *spxB* was approximately 2-fold higher in the *ritR* mutant when grown in Fe-CDM than when grown in Mn-CDM ($P < 0.05$) (Fig. 4B). Additionally, the *spxB* gene expression in the *ritR* mutant when grown in Fe-CDM was 2-fold

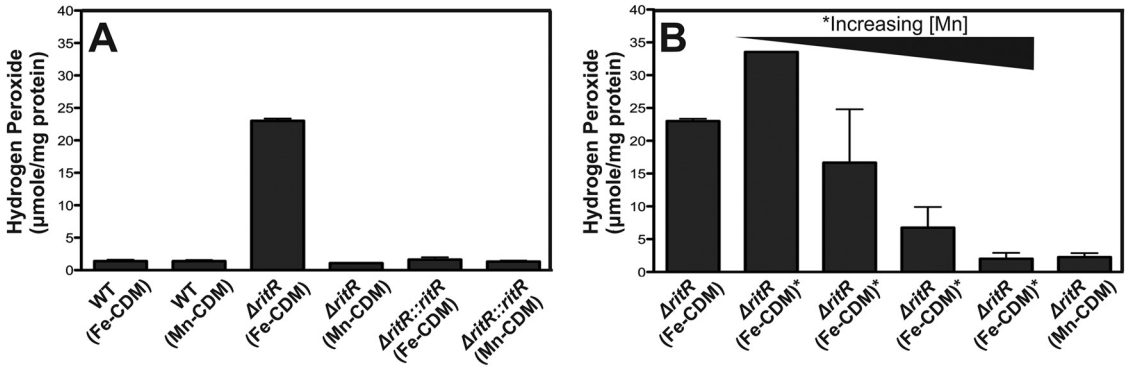

FIG 3 Hydrogen peroxide production from pneumococcal cells grown in different growth media. (A) Hydrogen production from D39 WT, isogenic deletion mutant (Δ*ritR*), and complemented (Δ*ritR*::*ritR*) strains grown in Fe-CDM compared to Mn-CDM. (B) Hydrogen peroxide production from the D39 Δ*ritR* strain grown in Mn-CDM and Fe-CDM supplemented with 0.1, 1, 10, and 100 μM Mn. Addition of Mn to the medium resulted in decreased hydrogen peroxide production. The results are shown as an average of three independent experiments, with the error bars representing the standard deviations, and the results were normalized with the cellular protein concentration. Samples were collected during the exponential phase of growth, with the exception of the Δ*ritR* strain when grown in Fe-CDM (the sample was collected during the lag phase of growth).

higher than expression in the wild-type and complemented strains when grown in both media ($P < 0.05$) (Fig. 4B).

A high-Fe environment can result in increased oxidative stress to bacteria (17, 29, 30). There are a number of ways bacteria combat this stress, most of which require NADPH as the ultimate source of reducing power to drive the detoxification of reactive oxygen species (31–33). In the pneumococcal genome, *gnd* is located directly upstream of *ritR* and encodes 6-phosphogluconate dehydrogenase, the second enzyme in the hexose monophosphate (HMP) shunt that diverts glucose 6-phosphate from glycolysis

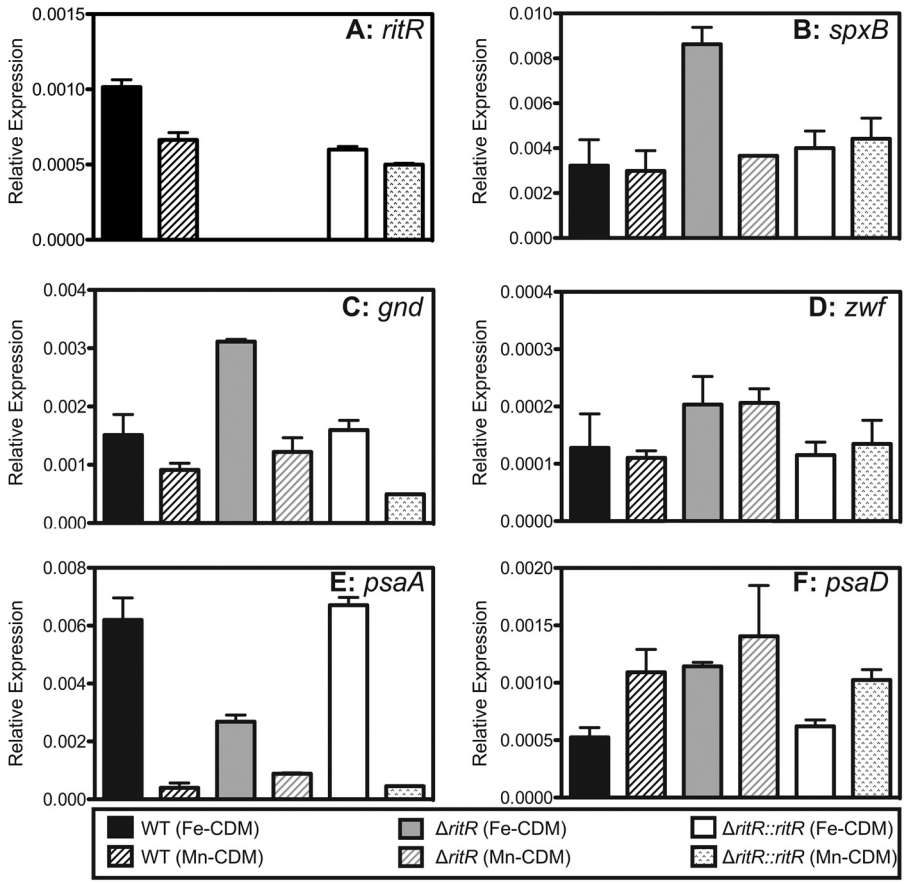

FIG 4 Relative gene expression of *ritR* (A), *spxB* (B), *gnd* (C), *zwf* (D), *psaA* (E), and *psaD* (F) from D39 WT, the isogenic deletion mutant (Δ*ritR*), and complemented (Δ*ritR*::*ritR*) cells when grown in either Fe-CDM or Mn-CDM. The relative gene expression was calculated using 16S RNA as the reference gene. All results represent the averages and standard deviations of three independent experiments.

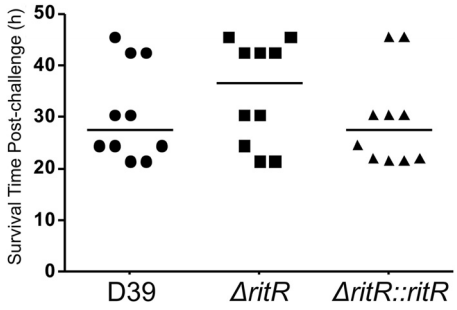

FIG 5 Survival time post-intraperitoneal challenge of female CD1 (Swiss) mice. The median mouse survival time postchallenge is represented by the horizontal line.

(the Embden-Meyerhof pathway) to the pentose phosphate pathway and generates NADPH in the process (20). The relative gene expression of *gnd* was higher in cells grown in Fe-CDM than in those grown in Mn-CDM, consistent with the hypothesis that a high-Fe environment increases oxidative stress on the bacteria. ($P < 0.05$) (Fig. 4C). Furthermore, the relative gene expression of *gnd* was approximately 3-fold higher in the *ritR* mutant when grown in Fe-CDM compared to growth in Mn-CDM and the wild-type and the complemented *ritR* mutant in both media ($P < 0.05$) (Fig. 4C). The first enzyme in the HMP shunt that also generates NADPH is glucose 6-phosphate dehydrogenase (Zwf). In Mn-CDM, the gene expression of *zwf* was approximately 2-fold higher in the *ritR* mutant than in the wild type and the complemented *ritR* mutant ($P < 0.05$) (Fig. 4D). Similarly, in Fe-CDM, the general trend indicated that *zwf* expression was higher in the *ritR* mutant than in the wild type and the complemented *ritR* mutant, although statistical significance was not met ($P = 0.15$) (Fig. 4D).

The gene encoding the metal-binding component of the manganese ABC transporter, *psaA*, was expressed at approximately 12-fold-higher levels in both the wild type and the complemented *ritR* mutant when the cells were grown in Fe-CDM than when they were grown in Mn-CDM ($P < 0.05$) (Fig. 4E). However, *psaA* was expressed at only 2-fold-higher levels in the *ritR* mutant when it was grown in Fe-CDM than when it was grown in Mn-CDM ($P < 0.05$) (Fig. 4E). In Fe-CDM, the *ritR* mutant expressed *psaA* at approximately 2-fold-lower levels than the wild-type and the complemented strain ($P < 0.05$) (Fig. 4E).

The putative thiol peroxidase, PsaD, has been thought to be involved in defense against oxidative stress (5). In general, the trend indicated slightly higher *psaD* gene expression in Mn-CDM than in Fe-CDM, with only the wild-type data reaching statistical significance (Fig. 4F). This could indicate that the enzyme is Mn regulated, as it is situated downsteam of the *psaBCA* operon. Furthermore, studies have shown that transcription of *psaD* from the *psaD* promoter is weaker than that from the *psaBCA* promoter (5, 34). In Fe-CDM, where oxidative stress levels are elevated, gene expression of *psaD* is approximately 2-fold higher in the *ritR* mutant than in the wild type and the complemented strain ($P < 0.05$) (Fig. 4F).

Virulence of a D39 Δ*ritR* deletion mutant in a mouse model of infection. Previous studies (35, 36) have suggested that RitR might have an important role in virulence. We used the *ritR* deletion mutant of *S. pneumoniae* D39 and compared its virulence with that of the otherwise isogenic wild-type and complemented strains. After intraperitoneal challenge, the average mouse survival time was slightly higher when inoculated with the *ritR* mutant than when inoculated with the wild type and the complemented *ritR* mutant (Fig. 5). This result was, however, not statistically significant, and all mice failed to survive past 2 days postinfection. Following an intraperitoneal infection, after 24 h, there was essentially no difference in the numbers of CFU of the pneumococcus recovered from blood (Fig. 6A), and this was also

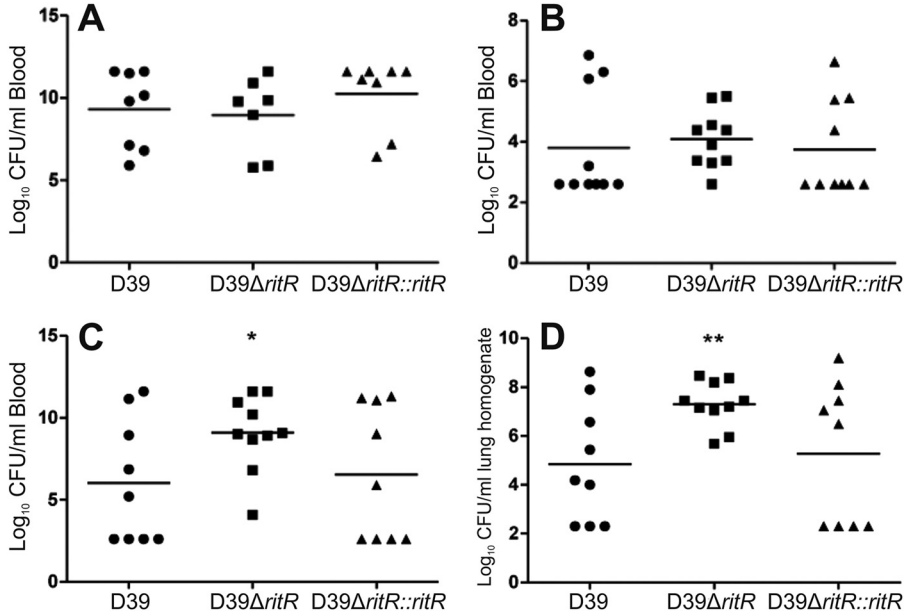

FIG 6 Numbers of pneumococci recovered from blood 24 h post-intraperitoneal challenge (A), blood 24 h post-intranasal challenge (B), blood 48 h post-intranasal challenge (C), and lungs 48 h post-intranasal challenge (D). *t* tests were performed for D39 versus D39 Δ*ritR* and D39 versus D39 Δ*ritR*::*ritR*; *, $P < 0.05$; **, $P < 0.01$.

the case following an intranasal challenge (Fig. 6B). However, at 48 h, there was actually an increased recovery of the *ritR* mutant compared to the wild-type and complemented strains from both blood and lungs (Fig. 6C and D, respectively). Taken together, these results indicate that RitR is not essential for pneumococcal survival in a mouse model of infection.

DISCUSSION

Manganese has been established for some time as a key transition metal ion for the growth and virulence of pneumococci (5, 37–39). This view is largely derived from the observation that the manganese ABC transporter PsaBCA is critical for the survival of *S. pneumoniae* (5, 8, 11), but more specifically, it is known that SodA is also essential for virulence (7). These observations support the view that Mn plays an important role as an antioxidant, potentially via a variety of mechanisms (7, 28, 39–42). In contrast to Mn, Fe is a promoter of oxidative stress, especially in combination with hydrogen peroxide, since this leads to the production of hydroxyl radicals via the Fenton reaction (43). This is potentially devastating for *S. pneumoniae*, since it produces hydrogen peroxide as the product of pyruvate oxidation during growth in the presence of oxygen. *S. pneumoniae* has a limited demand for Fe; the bacterium lacks a respiratory chain and hence possesses no cytochromes (20), although it does require iron for the formation of enzymes containing FeS clusters, including anaerobic ribonucleotide reductase (20). In addition, mutation of the genes encoding the ABC transporters required for iron acquisition (*piaABCD* and *piuBCDA*) leads to attenuation of *S. pneumoniae* in a murine model of infection (44, 45).

It has been established that coordinate RitR-dependent repression of expression of Fe uptake systems (25, 44–46) and the derepression of genes (*dps*) involved in protection against Fe and hydrogen peroxide stress appear to contribute to protection of pneumococci against the toxic effects of the Fenton reaction. As expected, we observed that loss of control of iron homeostasis and defense against Fe and peroxide led to susceptibility of the *ritR* mutant to Fe toxicity when the Fe/Mn ratio was high. We expected that Mn might rescue the mutant under these conditions, and this proved to be the case (Fig. 1B). However, the rescue of the *ritR* mutant by Mn in the presence of high Fe levels appears to be a consequence of a reduction in the level of intracellular iron (Fig. 2B). These data are consistent with the view that Mn protects *S. pneumoniae* by competing with Fe for transport into the bacterium. The Pia, Piu, and Pit transporters of *S. pneumoniae* are all paralogous to the SitABC family of transporters, which are established as transporters of both Mn(II) and Fe(III) (45–48). The ionic radius of Mn^{2+} (0.80 Å) is relatively close to those of Fe^{3+} (0.76 Å) and other divalent metal cations. Therefore, it is not uncommon for Mn^{2+} and other metal cations to be interchangeable in the metal-binding sites of proteins, as well as through cation transporters (40). In *Streptococcus pyogenes*, the iron transporter Siu, which is similar to Piu, can be inhibited by the addition of manganese (49). In *Streptococcus mutans*, the SloABC transporter can transport both manganese and iron (50). Increased Mn availability did not lead to a high intracellular concentration of the cation. This situation is probably the result of the action of the Mn efflux transporter MntE (51), which specifically removes Mn from the cytoplasm. Thus, it appears that the interplay between Fe and Mn may be similar to that which has been observed for Zn and Mn, which are tightly controlled by a combination of inducible uptake systems and efflux pumps (10). The Zn and Mn systems are connected at the level of uptake (Zn antagonizes the transport of Mn by the Psa transport system) and regulation of gene expression (Zn binding to the regulator PsaR leads to derepression of the Psa transport system) (6, 38). Similarly, Fe and Mn may be connected, but in a different way; Imlay and coworkers have shown that the protective effects of Mn may arise from its ability to substitute for ferrous iron in some enzymes. An example is ribulose-5-P epimerase in the pentose phosphate cycle. Such a substitution would render these enzymes more resistant to hydrogen peroxide (52). The number of enzymes in the cell whose metallation can change according to fluctuations in the Fe/Mn ratio is not known, but this may represent an additional mechanism to protect the cell against oxidative stress. Unlike Zn and Mn, there is no known efflux system for Fe, and thus, the RitR-dependent repression of transport and protection against excess Fe in the cytoplasm using Dps is the mechanism whereby the pro-oxidant effects of Fe are suppressed.

We also observed that rescue of the *ritR* mutant by Mn in high-Fe media was accompanied by a decrease in the steady-state level of H_2O_2 (Fig. 3B). This provides a second mechanism to suppress Fenton chemistry. The availability of oxygen means that *S. pneumoniae* can enhance its energy production beyond that available from conventional glycolysis; the NADH produced in glycolysis is oxidized by NADH oxidase (Nox) (12, 14). Although this reaction does not generate energy, its redox-balancing effect means that pyruvate, the end product of glycolysis, does not have to be used as an electron acceptor. The action of Nox makes pyruvate available for oxidation by pyruvate oxidase (SpxB), which generates acetyl-P and hydrogen peroxide. The generation of acetyl-P yields two additional ATP molecules per glucose molecule, compared to fermentation, which ends in lactate production. The outcome of this process is production of hydrogen peroxide. The altered level of H_2O_2 could be a consequence of decreased production of reactive oxygen species via pyruvate oxidase or increased removal of H_2O_2 via the thiol-peroxidase PsaD. Our data suggest that the Fe/Mn ratio in *S. pneumoniae* may be a critical factor in modulating the peroxide levels in pneumococci.

In spite of its clear requirement for protection against the effects of iron overload *in vitro*, our observations indicate that RitR is not critical for the survival of pneumococci in a murine model of infection. In previous studies, it was observed that recovery of a *ritR* mutant from the lungs of mice was significantly lower than recovery of the wild-type strain 48 h post-intransal challenge (25, 36). This contrasted with our results, in which recovery of the *ritR* mutant was greater (Fig. 6D). We cannot readily explain this apparent discrepancy, except that the experiments were conducted with different pneumococcal strains using distinct mouse models. Both these parameters are known to impact the behavior of pneumococci *in vivo*. Indeed, Ulijasz et al. (25) used cyclophosphamide-treated mice in order to enable an otherwise avirulent nonencapsulated pneumococcal strain to cause disease, while Throup et al. challenged mice with suspensions of serotype 3 pneumococci grown overnight on tryptic soy agar (36). In our model of infection, mice were challenged with pneumococci cultivated in serum broth, which optimizes capsule expression. The fact that the *ritR* mutant examined in this study seemed to survive so well in the mouse model may be a consequence of increased iron uptake; this has recently been shown to enhance biofilm formation, and hence, it may also improve survival in the lungs and blood (53).

ACKNOWLEDGMENTS

This research was supported Program Grant 565526 from the National Health and Medical Research Council (NHMRC) of Australia. J.C.P. is an NHMRC Australia Fellow.

REFERENCES

1. **Forrest JM, McIntyre PB, Burgess MA.** 2000. Pneumococcal disease in Australia. Commun. Dis. Intell. **24**:89–92.
2. **McCullers JA, Tuomanen EL.** 2001. Molecular pathogenesis of pneumococcal pneumonia. Front. Biosci. **6**:D877–D889.
3. **Williams BG, Gouws E, Boschi-Pinto C, Bryce J, Dye C.** 2002. Estimates of world-wide distribution of child deaths from acute respiratory infections. Lancet Infect. Dis. **2**:25–32.
4. **World Health Organization.** 2007. Pneumococcal conjugate vaccine for childhood immunization. WHO position paper. Wkly. Epidemiol. Rec. **82**:93–104.
5. **McAllister LJ, Tseng HJ, Ogunniyi AD, Jennings MP, McEwan AG, Paton JC.** 2004. Molecular analysis of the psa permease complex of *Streptococcus pneumoniae.* Mol. Microbiol. **53**:889–901.
6. **Johnston JW, Briles DE, Myers LE, Hollingshead SK.** 2006. Mn2+-dependent regulation of multiple genes in *Streptococcus pneumoniae* through PsaR and the resultant impact on virulence. Infect. Immun. **74**: 1171–1180.
7. **Yesilkaya H, Kadioglu A, Gingles N, Alexander JE, Mitchell TJ, Andrew PW.** 2000. Role of manganese-containing superoxide dismutase in oxidative stress and virulence of *Streptococcus pneumoniae.* Infect. Immun. **68**: 2819–2826.
8. **Tseng HJ, McEwan AG, Paton JC, Jennings MP.** 2002. Virulence of *Streptococcus pneumoniae*: PsaA mutants are hypersensitive to oxidative stress. Infect. Immun. **70**:1635–1639.
9. **Morona JK, Morona R, Miller DC, Paton JC.** 2002. *Streptococcus pneumoniae* capsule biosynthesis protein CpsB is a novel manganese-dependent phosphotyrosine-protein phosphatase. J. Bacteriol. **184**:577–583.
10. **McDevitt CA, Ogunniyi AD, Valkov E, Lawrence MC, Kobe B, McEwan AG, Paton JC.** 2011. A molecular mechanism for bacterial susceptibility to zinc. PLoS Pathog. **7**:e1002357. doi:10.1371/journal.ppat.1002357.
11. **Dintilhac A, Alloing G, Granadel C, Claverys JP.** 1997. Competence and virulence of *Streptococcus pneumoniae*: Adc and PsaA mutants exhibit a requirement for Zn and Mn resulting from inactivation of putative ABC metal permeases. Mol. Microbiol. **25**:727–739.
12. **Auzat I, Chapuy-Regaud S, Le Bras G, Dos Santos D, Ogunniyi AD, Le Thomas I, Garel JR, Paton JC, Trombe MC.** 1999. The NADH oxidase of *Streptococcus pneumoniae*: its involvement in competence and virulence. Mol. Microbiol. **34**:1018–1028.
13. **Higuchi M, Yamamoto Y, Kamio Y.** 2000. Molecular biology of oxygen tolerance in lactic acid bacteria: Functions of NADH oxidases and Dpr in oxidative stress. J. Biosci. Bioeng. **90**:484–493.
14. **Yu J, Bryant AP, Marra A, Lonetto MA, Ingraham KA, Chalker AF, Holmes DJ, Holden D, Rosenberg M, McDevitt D.** 2001. Characterization of the *Streptococcus pneumoniae* NADH oxidase that is required for infection. Microbiology **147**:431–438.
15. **Pericone CD, Park S, Imlay JA, Weiser JN.** 2003. Factors contributing to hydrogen peroxide resistance in *Streptococcus pneumoniae* include pyruvate oxidase (SpxB) and avoidance of the toxic effects of the Fenton reaction. J. Bacteriol. **185**:6815–6825.
16. **Ramos-Montanez S, Tsui HCT, Wayne KJ, Morris JL, Peters LE, Zhang F, Kazmierczak KM, Sham LT, Winkler ME.** 2008. Polymorphism and regulation of the *spxB* (pyruvate oxidase) virulence factor gene by a CBS-HotDog domain protein (SpxR) in serotype 2 *Streptococcus pneumoniae.* Mol. Microbiol. **67**:729–746.
17. **Imlay JA.** 2008. Cellular defenses against superoxide and hydrogen peroxide. Annu. Rev. Biochem. **77**:755–776.
18. **Daly MJ, Gaidamakova EK, Matrosova VY, Kiang JG, Fukumoto R, Lee DY, Wehr NB, Witeri GA, Berlett BS, Levine RL.** 2010. Small-molecule antioxidant proteome-shields in *Deinococcus radiodurans.* PLoS One **5**:e12570. doi:10.1371/journal.pone.0012570.
19. **Daly MJ, Gaidamakova EK, Matrosova VY, Vasilenko A, Zhai M, Venkateswaran A, Hess M, Omelchenko MV, Kostandarithes HM, Makarova KS, Wackett LP, Fedrickson JK, Ghosal D.** 2004. Accumulation of Mn(II) in Deinococcus radiodurans facilitates gamma-radiation resistance. Science **306**:1025–1028.
20. **Lanie JA, Ng WL, Kazmierczak KM, Andrzejewski TM, Davidsen TM, Wayne KJ, Tettelin H, Glass JI, Winkler ME.** 2007. Genome sequence of Avery's virulent serotype 2 strain D39 of *Streptococcus pneumoniae* and comparison with that of unencapsulated laboratory strain R6. J. Bacteriol. **189**:38–51.
21. **Hoskins J, Alborn WE, Arnold J, Blaszczak LC, Burgett S, DeHoff BS, Esterm ST, Fritz L, Fu DJ, Fuller W, Geringer C, Gilmour R, Glass JS, Khoka H, Kraft AR, Lagace RE, LeBlanc DJ, Lee LN, Lefkowitz EJ, Lu J, Matsushima P, McAhren SM, McHenney M, McLeaster K, Mundy CW, Nicas TI, Norris FH, O'Gara M, Peery RB, Robertson GT, Rockey P, Sun PM, Winkler ME, Yang Y, Young-Bellido M, Zhao GS, Sook CA, Baltz RH, Jaskunas SR, Rosteck PR, Skatrud PL, Glass JI.** 2001. Genome of the bacterium *Streptoccus pneumoniae* strain R6. J. Bacteriol. **183**:5709–5717.
22. **Tettelin H, Nelson KE, Paulsen IT, Eisen JA, Read TD, Peterson S, Heidelberg J, DeBoy RT, Haft DH, Dodson RJ, Durkin AS, Gwinn M, Kolonay JF, Nelson WC, Peterson JD, Umayam LA, White O, Salzberg SL, Lewis MR, Radune D, Holtzapple E, Khouri H, Wolf AM, Utterback TR, Hansen CL, McDonald LA, Feldblyum TV, Venter JC, Dougherty BA, Morrison DA, Hollingshead SK, Fraser CM.** 2001. Complete genome sequence of a virulent isolate of *Streptococcus pneumoniae.* Science **293**:498–506.
23. **Pulliainen AT, Haataja S, Kahkonen S, Finne J.** 2003. Molecular basis of H2O2 resistance mediated by streptococcal Dpr: demonstration of the functional involvement of the putative ferroxidase center by site-directed mutagenesis in *Streptococcus suis.* J. Biol. Chem. **278**:7996–8005.
24. **Park S, You X, Imlay JA.** 2004. Dps protein protects *E.* coli against oxidative DNA damage from micromolar levels of H2O2, p 383. Abstr. 104th Gen. Meet. Am. Soc. Microbiol. American Society for Microbiology, Washington, DC.
25. **Ulijasz AT, Andes DR, Glasner JD, Weisblum B.** 2004. Regulation of iron transport in *Streptococcus pneumoniae* by RitR, an orphan response regulator. J. Bacteriol. **186**:8123–8136.
26. **Vanderijn I, Kessler RE.** 1980. Growth characteristics of group A streptococci in a new chemically defined medium. Infect. Immun. **27**:444–448.
27. **Yother J, McDaniel LS, Briles DE.** 1986. Transformation of encapsulated *Streptococcus pneumoniae.* J. Bacteriol. **168**:1463–1465.
28. **Anjem A, Varghese S, Imlay JA.** 2009. Manganese import is a key element of the OxyR response to hydrogen peroxide in *Escherichia coli.* Mol. Microbiol. **72**:844–858.
29. **Imlay JA.** 2006. Iron-sulphur clusters and the problem with oxygen. Mol. Microbiol. **59**:1073–1082.
30. **Anjem A, Imlay JA.** 2012. Mononuclear iron enzymes are primary targets of hydrogen peroxide stress. J. Biol. Chem. **287**:15544–15556.
31. **Minard KI, McAlister-Henn L.** 2005. Sources of NADPH in yeast vary with carbon source. J. Biol. Chem. **280**:39890–39896.
32. **Shi F, Li YF, Li Y, Wang XY.** 2009. Molecular properties, functions, and potential applications of NAD kinases. Acta Biochim. Biophys. Sin. **41**: 352–361.
33. **Singh R, Mailloux RJ, Puiseux-Dao S, Appanna VD.** 2007. Oxidative stress evokes a metabolic adaptation that favors increased NADPH synthesis and decreased NADH production in *Pseudomonas fluorescens.* J. Bacteriol. **189**:6665–6675.
34. **Novak R, Braun JS, Charpentier E, Tuomanen E.** 1998. Penicillin tolerance genes of *Streptococcus pneumoniae*: the ABC-type manganese permease complex Psa. Mol. Microbiol. **29**:1285–1296.
35. **Ulijasz AT, Falk SP, Weisblum B.** 2009. Phosphorylation of the RitR DNA-binding domain by a Ser-Thr phosphokinase: implications for global gene regulation in the streptococci. Mol. Microbiol. **71**:382–390.
36. **Throup JP, Koretke KK, Bryant AP, Ingraham KA, Chalker AF, Ge YG, Marra A, Wallis NG, Brown JR, Holmes DJ, Rosenberg M, Burnham MKR.** 2000. A genomic analysis of two-component signal transduction in *Streptococcus pneumoniae.* Mol. Microbiol. **35**:566–576.
37. **Janulczyk R, Ricci S, Bjorck L.** 2003. MtsABC is important for manganese and iron transport, oxidative stress resistance, and virulence of *Streptococcus pyogenes.* Infect. Immun. **71**:2656–2664.
38. **Kloosterman TG, Witwicki RM, van der Kooi-Pol MM, Bijlsma JJE, Kuipers OP.** 2008. Opposite effects of Mn2+ and Zn2+ on PsaR-mediated expression of the virulence genes *pcpA*, *prtA*, and *psaBCA* of *Streptococcus pneumoniae.* J. Bacteriol. **190**:5382–5393.
39. **Ogunniyi AD, Mahdi LK, Jennings MP, McEwan AG, McDevitt CA, Van der Hoek MB, Bagley CJ, Hoffmann P, Gould KA, Paton JC.** 2010. Central role of manganese in regulation of stress responses, physiology,

and metabolism in *Streptococcus pneumoniae.* J. Bacteriol. **192**:4489–4497.
40. **Jakubovics NS, Jenkinson HF.** 2001. Out of the iron age: new insights into the critical role of manganese homeostasis in bacteria. Microbiology **147**:1709–1718.
41. **Jakubovics NS, Smith AW, Jenkinson HF.** 2002. Oxidative stress tolerance is manganese (Mn2+) regulated in *Streptococcus gordonii.* Microbiology **148**:3255–3263.
42. **McEwan AG.** 2009. New insights into the protective effect of manganese against oxidative stress. Mol. Microbiol. **72**:812–814.
43. **Imlay JA, Chin SM, Linn S.** 1988. Toxic DNA damage by hydrogen peroxide through the Fenton reaction in vivo and in vitro. Science **240**:640–642.
44. **Brown JS, Gilliland SM, Holden DW.** 2001. A *Streptococcus pneumoniae* pathogenicity island encoding an ABC transporter involved in iron uptake and virulence. Mol. Microbiol. **40**:572–585.
45. **Brown JS, Gilliland SM, Ruiz-Albert J, Holden DW.** 2002. Characterization of pit, a *Streptococcus pneumoniae* iron uptake ABC transporter. Infect. Immun. **70**:4389–4398.
46. **Whalan RH, Funnell SGP, Bowler LD, Hudson MJ, Robinson A, Dowson CG.** 2006. Distribution and genetic diversity of the ABC transporter lipoproteins PiuA and PiaA within *Streptococcus pneumoniae* and related streptococci. J. Bacteriol. **188**:1031–1038.
47. **Ikeda JS, Janakiraman A, Kehres DG, Maguire ME, Slauch JM.** 2005. Transcriptional regulation of sitABCD of *Salmonella enterica* serovar Typhimurium by MntR and Fur. J. Bacteriol. **187**:912–922.
48. **Sabri M, Leveille S, Dozois CM.** 2006. A SitABCD homologue from an avian pathogenic *Escherichia coli* strain mediates transport of iron and manganese resistance to hydrogen peroxide. Microbiology **152**:745–758.
49. **Montanez GE, Neely MN, Eichenbaum Z.** 2005. The streptococcal iron uptake (Siu) transporter is required for iron uptake and virulence in a zebrafish infection model. Microbiology **151**:3749–3757.
50. **Paik S, Brown A, Munro CL, Cornelissen CN, Kitten T.** 2003. The sloABCR operon of *Streptococcus mutans* encodes an Mn and Fe transport system required for endocarditis virulence and its Mn-dependent repressor. J. Bacteriol. **185**:5967–5975.
51. **Rosch JW, Gao G, Ridout G, Wang YD, Tuomanen EI.** 2009. Role of the manganese efflux system *mntE* for signalling and pathogenesis in *Streptococcus pneumoniae.* Mol. Microbiol. **72**:12–25.
52. **Sobota JM, Imlay JA.** 2011. Iron enzyme ribulose-5-phosphate 3-epimerase in *Escherichia coli* is rapidly damaged by hydrogen peroxide but can be protected by manganese. Proc. Natl. Acad. Sci. U. S. A. **108**:5402–5407.
53. **Trappetti C, Potter AJ, Paton AW, Oggioni MR, Paton JC.** 2011. LuxS mediates iron-dependent biofilm formation, competence, and fratricide in *Streptococcus pneumoniae.* Infect. Immun. **79**:4550–4558.